

Optical spectroscopy shows that the normal state of URu₂Si₂ is an anomalous Fermi liquid

Urmaz Nagel^a, Taaniel Wleksin^a, Toomas Rõõm^a, Ricardo P. S. M. Lobo^b, Pascal Lejay^c, Christopher C. Homes^d, Jesse S. Hall^e, Alison W. Kinross^e, Sarah K. Purdy^e, Tim Munsie^e, Travis J. Williams^e, Graeme M. Luke^{e,f}, and Thomas Timusk^{e,f,1}

^aNational Institute of Chemical Physics and Biophysics, 12618 Tallinn, Estonia; ^bLaboratoire de Physique et d'Étude des Matériaux, École Supérieure de Physique et de Chimie Industrielles de la Ville de Paris, ParisTech, Université Pierre et Marie Curie, Centre National de la Recherche Scientifique, 75005 Paris, France; ^cInstitut Néel, Centre National de la Recherche Scientifique/Université Joseph Fourier, 38042 Grenoble Cedex 9, France; ^dCondensed Matter Physics and Materials Science Department, Brookhaven National Laboratory, Upton, NY 11780; ^eDepartment of Physics and Astronomy, McMaster University, Hamilton, ON, Canada L8S 4M1; and ^fCanadian Institute for Advanced Research, Toronto, ON, Canada M5G 1Z8

Edited* by J. C. Seamus Davis, Cornell University, Ithaca, NY, and approved October 2, 2012 (received for review May 16, 2012)

Fermi showed that, as a result of their quantum nature, electrons form a gas of particles whose temperature and density follow the so-called Fermi distribution. As shown by Landau, in a metal the electrons continue to act like free quantum mechanical particles with enhanced masses, despite their strong Coulomb interaction with each other and the positive background ions. This state of matter, the Landau–Fermi liquid, is recognized experimentally by an electrical resistivity that is proportional to the square of the absolute temperature plus a term proportional to the square of the frequency of the applied field. Calculations show that, if electron–electron scattering dominates the resistivity in a Landau–Fermi liquid, the ratio of the two terms, b , has the universal value of $b = 4$. We find that in the normal state of the heavy Fermion metal URu₂Si₂, instead of the Fermi liquid value of 4, the coefficient $b = 1 \pm 0.1$. This unexpected result implies that the electrons in this material are experiencing a unique scattering process. This scattering is intrinsic and we suggest that the uranium f electrons do not hybridize to form a coherent Fermi liquid but instead act like a dense array of elastic impurities, interacting incoherently with the charge carriers. This behavior is not restricted to URu₂Si₂. Fermi liquid-like states with $b \neq 4$ have been observed in a number of disparate systems, but the significance of this result has not been recognized.

hidden order | resistance | infrared conductivity | resonant scattering

Among the heavy Fermion metals, URu₂Si₂ is one of the most interesting: it displays, in succession, no fewer than four different behaviors. As is shown in Fig. 1, where the electrical resistivity is plotted as a function of temperature, at 300 K the material is a very bad metal in which the conduction electrons are incoherently scattered by localized uranium f electrons. Below $T_K \sim 75$ K, the resistivity drops and the material resembles a typical heavy Fermion metal (1–3). At $T_0 = 17.5$ K the “hidden-order” phase transition gaps a substantial portion of the Fermi surface but the nature of the order parameter is not known. A number of exotic models for the ordered state have been proposed (4–7), but there is no definitive experimental evidence to support them. Finally, at 1.5 K URu₂Si₂ becomes an unconventional superconductor. The electronic structure, as shown by both angle-resolved photoemission experiments (8) and band-structure calculations (9) is complicated, with several bands crossing the Fermi surface. To investigate the nature of the hidden-order state we focus on the normal state just above the transition. This approach has been used in the high-temperature superconductors where the normal state shows evidence of discrete frequency magnetic excitations that appear to play the role that phonons play in normal superconductors (10). The early optical experiments of Bonn et al. (11) showed that URu₂Si₂ at 20 K, above the hidden order transition, has an infrared spectrum consisting of a narrow Drude peak and a strong incoherent background. The large electronic specific heat just

above the transition pointed to the presence of heavy carriers with a mass $m^* = 25m_e$ (2). However, recent scanning tunneling microscopy (STM) experiments contradict this model (12, 13). Schmidt et al. (12) find a light band crossing the Fermi surface above 17.5 K turning into a hybridized heavy band only below the hidden-order transition. This finding contradicts the conventional view that mass builds up gradually below T_K , although there have been recent reports of some hybridization occurring in the 25–30 K region by Park et al. (14) and Levallois et al. (15), but the reported effects are weak and perhaps not resolved by all spectroscopies. We can test the development of mass by carefully tracking the Drude weight as a function of temperature with optical spectroscopy. The Drude weight is a quantitative measure of the effective mass of the carriers. Before turning to an optical investigation of the normal state of URu₂Si₂, we will review briefly what is known from optical spectroscopy of other metallic systems at low temperature.

In pure metals, at high temperature the dominant source of resistance is the electron–phonon interaction, giving rise to the familiar linear temperature-dependence of the electrical resistance. At low temperature the phonon contribution weakens and the resistance varies as T^2 , where T is the absolute temperature. Gurzhi showed that under rather general conditions, the resistivity of a pure metal at low temperature is given by $\rho(\omega, T) = A'[\hbar\omega^2 + 4\pi^2(k_B T)^2]$, where ω is the frequency of the field used to measure the resistivity, and A' a constant that varies from material to material (16). This formula is valid for three-dimensional systems, as long as Galilean invariance is broken by the lattice, and the Fermi surface is not convex and simply connected (16–22), and then in the high-frequency regime when $\omega \gg 1/\tau^{sp}(\omega, T)$ with $1/\tau^{sp}(\omega, T)$ being the single-particle scattering rate. In the dc limit, the resistivity behaves as $\rho(T) = AT^2$, if umklapp scattering is allowed. Notice that although the coefficients A and A' contain different combinations of umklapp and normal scattering amplitudes, they are related as $A = 4\pi^2 A'$ if umklapp scattering dominates over the normal one. We prefer to introduce a parameter b , which we define as $b = A/(A'\pi^2)$. Then, if the Gurzhi resistivity formula is valid, $b = 4$. A source of confusion in the literature is the formula for the single-particle scattering rate $1/\tau^{sp}$ within Fermi liquid theory $1/\tau^{sp}(\omega, T) = A'[(\hbar\omega^2 + \pi^2(k_B T)^2)]$ that is sometimes used to describe the resistivity. This formula does not apply here and, to be general, we will use the parameter b as a quantity that is measured by comparing the frequency and temperature terms in Gurzhi's

Author contributions: U.N., T.U., T.R., R.P.S.M.L., C.C.H., J.S.H., A.W.K., S.K.P., T.M., G.M.L., and T.T. performed research; P.L., T.J.W., and G.M.L. contributed new reagents/analytic tools; A.W.K. and T.M. analyzed data; and T.T. wrote the paper.

The authors declare no conflict of interest.

*This Direct Submission article had a prearranged editor.

¹To whom correspondence should be addressed. E-mail: timusk@mcmaster.ca.

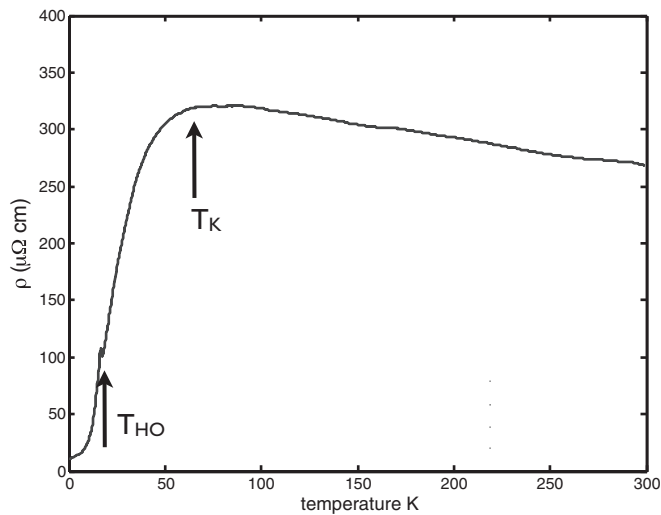


Fig. 1. The dc resistivity of URu_2Si_2 as a function of temperature. Unlike ordinary metals, the resistivity rises as the temperature is lowered below 300 K to reach a maximum at around 75 K, referred to as the Kondo temperature, T_K . Below this temperature the resistivity drops dramatically and the system acquires a Drude peak at low frequency, a defining property of a material with metallic conductivity. This change of resistivity slope at T_K is the signature of a heavy Fermion system, where the conduction electrons hybridize with f electrons to form massive carriers. In URu_2Si_2 , this process is interrupted at 17.5 K by a phase transition, called the hidden-order transition, where a portion of the Fermi surface is gapped. Our aim in this work is to investigate the electrodynamics of this system just above the hidden-order state.

formula, in the same energy range $\hbar\omega \sim k_B T$. Although the focus of this report is an accurate determination of b in the normal state above the hidden-order transition of URu_2Si_2 , it is useful to look at previous work, where the quantity b can be extracted from the measured optical resistivity $\rho(\omega, T)$ and, in some cases, the dc resistivity $\rho(T)$. These are challenging experiments because Fermi liquid scattering, in most metals, is a low-temperature phenomenon and, therefore, to stay in the energy range where the temperature dependence of the resistivity is examined, the optical measurements have to be carried out in the very far infrared, an experimentally difficult region. Nevertheless, a search of the literature turns up several examples.

The first report of a discrepancy of the ratio of the amplitudes of the frequency and temperature terms in a Fermi liquid was a report by Sulewski et al. (23) on the infrared properties of the heavy Fermion material UPt_3 . Instead of the expected value of $b = 4$, they reported an experimental upper limit of $b = 1$. Since then a number of studies have presented both T^2 and ω^2 dependencies of the optical scattering on the same material (24–26). A summary of these is given in Table 1. In some cases, the authors have not calculated the ratio A/A' , in which case we have made an estimate

Table 1. Summary of experimental measurements of the ratio b of temperature and frequency terms for some Fermi liquids

Material	T_{max} (meV)	ω_{max} (meV)	b	Source
UPt_3	1	1	<1	(23)
CePd_3			1.3	(23)
$\text{Ce}_{0.95}\text{Ca}_{0.05}\text{TiO}_{3.04}$	25	100	1.72	(24)
Cr	28	370	2.5	(25)
$\text{Nd}_{0.95}\text{TiO}_4$	24	50	1.1	(26)
URu_2Si_2	2	10	1.0	Present work

T_{max} and ω_{max} indicate the upper limit of the measured quadratic behavior of $\rho(T)$ and $\rho(\omega)$, respectively.

from the published curves. We have also tabulated the approximate maximum temperatures and frequencies where the quadratic dependence is observed. It is important that these overlap to some extent. The overall conclusion one can draw from this table is that in no case has the expected canonical Fermi liquid behavior with $b = 4$ been observed experimentally. Additional examples of non-Fermi liquid behavior are given in a review by Dressel (27).

Results

Fig. 2 shows the optical conductivity between 20 and 75 K, the region where coherence develops, as shown by the appearance of a Drude peak below 15 meV, which narrows as the temperature is lowered. Above 75 K the optical conductivity is frequency- and temperature-independent. Interestingly, we find that in the temperature range 75 K to 20 K the area under the Drude peak is temperature-independent, with a plasma frequency of ~ 400 meV. This finding is a signature that m^* is constant in this region of temperatures. A distinct minimum develops between the Drude peak and the high-frequency saturation value. We suggest this minimum is a pseudohybridization gap normally associated with the formation of the Kondo lattice but not fully formed in this material above 17.5 K. There is a simple relationship between the Kondo temperature T_K , the effective mass m^* and the gap V_K : $m^*/m_e = (V_K/k_B T_K)^2$ (17, 28). Estimating $T_K = 75$ K from the temperature where the Drude peak first appears, and taking $V_K = 15 \pm 5$ meV, we find $m^*/m_e = 5 \pm 2$, which is lower than what is estimated from specific heat measurements (2) but not in disagreement with recent STM (12) or optical (15) data. We note here that the hybridization gap acts like the pseudogap in the cuprates; its frequency does not change with temperature but fills in gradually as the temperature is raised. In addition, the spectral weight lost in the gap region is not recovered by the Drude peak or in the spectral region immediately above the gap. The inset in Fig. 2 shows the accumulated spectral weight at the five temperatures. All of the curves cross at 15 meV, showing that the Drude weight is conserved in the temperature range from 20 to 75 K. On the other hand, spectral weight is lost above this frequency range as the temperature is lowered. These behaviors are inconsistent with a simple picture of an effective mass resulting from an inelastic interaction with a bosonic spectrum.

To examine quasiparticle damping above the hidden-order transition, we apply an extended Drude model to the conductivity:

$$\sigma(T, \omega) = \frac{\omega_p^2}{4\pi} \frac{1}{1/\tau^{op}(\omega) - i\omega(1 + \lambda(\omega))}, \quad [1]$$

where $\omega_p^2 = 4\pi n e^2 / m_e$ is the plasma frequency squared, $1/\tau^{op}(\omega) = \frac{\omega_p^2}{4\pi} \text{Re}(1/\sigma(\omega))$, the optical scattering rate, and $1 + \lambda(\omega) = m^*/m_e$ is the mass enhancement. Optical phonons at 13.5 and 46.9 meV have been subtracted from the measured conductivity. The renormalized optical scattering rate, $1/\tau^* = 1/\tau^{op}/(m^*/m_e)$, is shown in Fig. 3A, where we have used a plasma frequency of $\omega_p^* = \omega_p / \sqrt{m^*/m_e} = 418$ meV, evaluated from the Drude weight. As the temperature exceeds T_K , here taken as 75 K, the frequency-dependence below 14 meV is replaced by uniform temperature- and frequency-independent scattering. We also note that the low-frequency scattering above 20 K is incoherent in the sense that $1/\tau^* > \omega$ but, significantly, the condition reverses at 20 K, near the temperature of the hidden order transition.

We next turn to the optical resistivity, defined as $\rho(\omega) = \text{Re}[1/\sigma(\omega)]$, where $\sigma(\omega)$ is the complex conductivity. We used the “refined reflectivity” (*Materials and Methods*) to calculate this quantity, as plotted in Fig. 3B at three temperatures, because we are focusing on temperatures just above the phase transition. The zero frequency limit of $\rho(\omega)$ is the dc resistivity, which as mentioned above, has been adjusted to agree with the measured

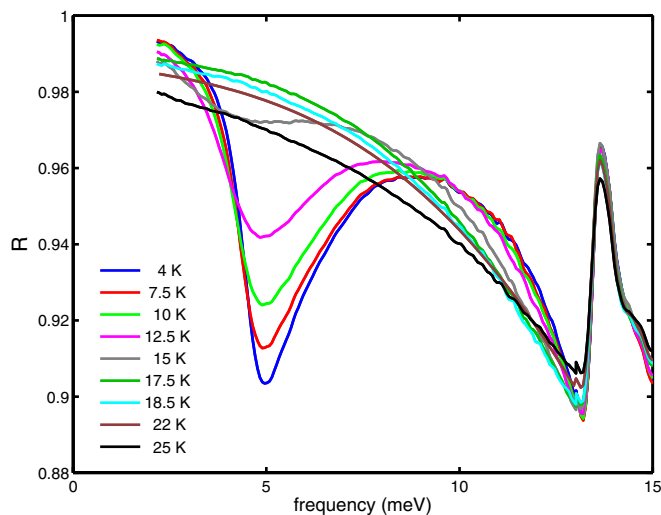


Fig. 6. “Refined” reflectance of URu_2Si_2 obtained by first measuring a series of spectra at different temperatures T and then dividing the spectra with one measured at a reference temperature T_{ref} . All this is done without moving the sample stage. The resulting temperature ratios are smooth without interference artifacts. Then, these smooth ratios are multiplied by the estimate to the absolute spectrum at T_{ref} shown in Fig. 4. The resulting spectra shown in the figure are a low noise approximation to the true absolute spectra of URu_2Si_2 . Of all of the spectra shown, only the one at $T_{ref} = 22$ K is a polynomial fit; all of the others show actual measured data.

At long wavelengths, a simple procedure which we call “refined thermal reflectance” was used to cancel out interference artifacts (32) below 13 meV. The procedure involves the following steps. We have found that the

interference artifacts seen in the absolute experimental spectrum (Fig. 5) are related to the movement of the sample stage. To overcome this problem, we measure the reflected spectra over a narrow temperature range without moving the sample stage, typically from 4 K to 25 K. Using one of the spectra as a reference, we record the ratios of the spectra at the various temperatures to the spectrum at the reference temperature. To obtain a low-noise absolute reflectance, we use the gold-overcoating technique to get an estimate of the absolute reflectance at the reference temperature. Because the sample is moved in this process this absolute spectrum is contaminated by interference artifacts. To eliminate these artifacts, we fit the absolute reflectance at the reference temperature with a cubic polynomial, a curve labeled “cubic fit” in Fig. 5. This smoothed spectrum is then used as a reference spectrum to calculate absolute spectra at all other temperatures. It is clear that the smoothing procedure hides any sharp structure in the reference spectrum. However, any new sharp structure that appears as the temperature is changed will be present at full resolution. The final refined spectra are shown in Fig. 6. This procedure is well-suited to the discovery of new spectral features that appear at phase transitions, for example the prominent minimum at 5 meV, because of the hidden-order gap. The measured refined reflectance was converted to an optical conductivity by Kramers–Kronig analysis. At low frequency, below 4 meV, a Drude response was assumed where we used the measured dc resistivity to determine the amplitude of the Drude peak and the absorption at our lowest measured infrared frequency to determine the width. At high frequency, beyond 7 eV, we used the results of Degiorgi et al. (33).

ACKNOWLEDGMENTS. We thank K. Behnia and T. Matsuda for supplying us with unpublished data. This work was supported by the Natural Science and Engineering Research Council of Canada and the Canadian Institute for Advanced Research. Work in Tallinn was supported by the Estonian Ministry of Education and Research under Grant SF0690029s09 and the Estonian Science Foundation under Grants ETF8170 and ETF8703; work in Paris was supported by the Agence Nationale de la Recherche under Grant BLAN07-1-183876 GAPSUPRA.

- Palstra TTM, et al. (1985) Superconducting and magnetic transitions in the heavy-fermion system URu_2Si_2 . *Phys Rev Lett* 55(24):2727–2730.
- Maple MB, et al. (1986) Partially gapped Fermi surface in the heavy-electron superconductor URu_2Si_2 . *Phys Rev Lett* 56(2):185–188.
- Palstra TTM, Menovsky AA, Mydosh JA (1986) Anisotropic electrical resistivity of the magnetic heavy-Fermion superconductor URu_2Si_2 . *Phys Rev B Condens Matter* 33(9): 6527–6530.
- Chandra P, Coleman P, Mydosh JA, Tripathi V (2002) Hidden orbital order in the heavy Fermion metal URu_2Si_2 . *Nature* 417(6891):831–834.
- Varma CM, Zhu L (2006) Helicity order: Hidden order parameter in URu_2Si_2 . *Phys Rev Lett* 96(3):036405.
- Hauke K, Kotliar G (2009) Arrested Kondo effect and hidden order in URu_2Si_2 . *Nat Phys* 5:796–799.
- Balatsky AV et al. (2009) Incommensurate spin resonance in URu_2Si_2 . *Phys Res B* 79(21):214413.
- Santander-Syro AF, et al. (2009) Fermi-surface instability at the hidden-order transition of URu_2Si_2 . *Nat Phys* 5:637.
- Oppeneer PM, et al. (2010) Electronic structure theory of the hidden-order material URu_2Si_2 . *Phys Rev B* 82:205103.
- Carbotte JP, Timusk T, Hwang J (2011) Bosons in high-temperature superconductors: An experimental survey. *Rep Prog Phys* 74:066501.
- Bonn DA, Garrett JD, Timusk T (1988) Far-infrared properties of URu_2Si_2 . *Phys Rev Lett* 61(11):1305–1308.
- Schmidt AR, et al. (2010) Imaging the Fano lattice to ‘hidden order’ transition in URu_2Si_2 . *Nature* 465(7298):570–576.
- Aynajian P, et al. (2010) Visualizing the formation of the Kondo lattice and the hidden order in URu_2Si_2 . *Proc Natl Acad Sci USA* 107(23):10383–10388.
- Park WK, et al. (2012) Observation of the hybridization gap and fano resonance in the Kondo lattice URu_2Si_2 . *Phys Rev Lett* 108(24):246403.
- Levallois J, et al. (2011) Hybridization gap and anisotropic far-infrared optical conductivity of URu_2Si_2 . *Phys Rev B* 84:184420.
- Gurzhi RN (1959) Mutual electron correlations in metal optics. *Sov Phys JETP* 35: 673–675.
- Millis AJ, Lee PA (1987) Large-orbital-degeneracy expansion for the lattice Anderson model. *Phys Rev B Condens Matter* 35(7):3394–3414.
- Rosch A, Howell PC (2005) Zero-temperature optical conductivity of ultraclean Fermi liquids and superconductors. *Phys Rev B* 72:104510.
- Jacko AC, Fjærestad JO, Powell BJ (2009) Unified explanation of the Kadowaki-Woods ratio in strongly correlated metals. *Nat Phys* 5:422–425.
- Maslov DL, Chubukov AV (2012) First-Matsubara-frequency rule in a Fermi liquid. II. Optical conductivity and comparison to experiment. *Phys Rev B* 86:155137.
- Maslov DL, Yudson VI, Chubukov AV (2011) Resistivity of a non-Galilean-invariant Fermi liquid near Pomeranchuk quantum criticality. *Phys Rev Lett* 106(10):106403.
- Pal HK, Yudson VI, Maslov DL (2011) Resistivity of non-Galilean-invariant Fermi- and non-Fermi liquids. *Phys Rev Lett* 106(10):106403.
- Sulewski PE, et al. (1988) Far-infrared absorptivity of UPT_3 . *Phys Rev* 38(8):5338–5352.
- Katsufuji T, Tokura Y (1999) Frequency and temperature dependence of conductivity for perovskite titanates. *Phys Rev B* 60:7673–7676.
- Basov DN, Singley EJ, Dordevic SV (2002) Sum rules and electrodynamics of high- T_c cuprates in the pseudogap state. *Phys Rev B* 65:054516.
- Yang J, Hwang J, Timusk T, Sefat AS, Gredan JE (2006) Temperature-dependent optical spectroscopy studies of $\text{Nd}_{1-x}\text{TiO}_3$. *Phys Rev B* 73:195125.
- Dressel M (2011) Quantum criticality in organic conductors? Fermi liquid versus non-Fermi-liquid behaviour. *J Phys Condens Matter* 23(29):293201.
- Dordevic SV, Basov DN, Dilley NR, Bauer ED, Maple MB (2001) Hybridization gap in heavy fermion compounds. *Phys Rev Lett* 86(4):684–687.
- Hwang J, Timusk T, Schachinger E, Carbotte JP (2007) Evolution of the bosonic spectral density of the high-temperature superconductor $\text{Bi}_2\text{Sr}_2\text{CaCu}_2\text{O}_{8-x}$. *Phys Rev B* 75:144508.
- Matsuda TD, et al. (2012) Details of sample dependence and transport properties of URu_2Si_2 . *J Phys Soc Jpn* 80:114710.
- Homes CC, Reedyk MA, Cradles DA, Timusk T (1993) Technique for measuring the reflectance of irregular, submillimeter-sized samples. *Appl Opt* 32(16):2976–2983.
- Purdy S (2010) Optical spectroscopy of URu_2Si_2 : A search for new features. MS thesis (McMaster University, Hamilton, ON, Canada).
- Degiorgi L, et al. (1997) The electrodynamic response of heavy-electron materials with magnetic phase transitions. *Z Phys B* 102:367.